Structure and Optical Property Evolutions in PbM(PO$_4$)X (M = Zn, Sn; X = halogen): SHG Effect and Birefringence

Xiao-Bao Li[a], Chun-Li Hu[a], Fang Kong[*,a], Jiang-Gao Mao[a]

[a] State Key Laboratory of Structural Chemistry, Fujian Institute of Research on the Structure of Matter, Chinese Academy of Sciences, Fuzhou 350002, P. R. China.

E-mail: kongfang@fjirsm.ac.cn

Table of Contents

Table S1. Crystal data and refinement details of the four crystals.

Formula	PbZn(PO$_4$)F (**1**)	PbSn(PO$_4$)Cl (**2**)	PbSn(PO$_4$)Br (**3**)	PbSn(PO$_4$)I (**4**)
F W	386.53	456.30	500.76	547.75
Temperature	294.56(10) K	293(2) (K)	281.8(5) (K)	296.59(10) (K)
Crystal system	Orthorhombic	Monoclinic	Monoclinic	Triclinic
Space group	*Pna2*$_1$	*P2*$_1$/*n*	*P2*$_1$/*n*	*P*-1
a (Å)	8.9845(10)	8.3519(2)	8.4780(9)	4.8059(6)
b (Å)	9.3813(13)	4.72080(10)	4.7595(5)	8.1218(9)
c (Å)	4.8212(6)	14.5277(3)	15.0060(16)	8.6719(10)
α (deg)/°	90.00	90.00	90.00	109.324(10)
β (deg)/°	90.00	101.299(2)	101.898(10)	91.471(10)
γ (deg)/°	90.00	90.00	90.00	90.588(10)
V (Å^3)	406.36(9)	561.69(2)	592.50(11)	319.00(8)
Z	4	4	4	2
Flack factor	-0.023(14)	/	/	/
ρ_{calc} (g/cm^3)	6.318	5.396	5.614	5.698
μ (mm^{-1})	47.595	35.057	39.527	35.258
GOF on F^2	1.013	1.064	0.933	1.132
R$_1$, wR$_2$[I>2σ (I)][a]	0.0331, 0.0686	0.0490, 0.1273	0.0466, 0.1192	0.0747, 0.2182
R$_1$, wR$_2$ (all data)	0.0366, 0.0715	0.0510, 0.1287	0.0508, 0.1274	0.0786, 0.2211

[a] $R_1 = \Sigma||F_o| -|F_c||/\Sigma|F_o|$, $wR_2 = \{\Sigma w[(F_o)^2 -(F_c)^2]^2/\Sigma w[(F_o)^2]^2\}^{1/2}$

Table S2. Selected bond lengths (Å) for the four crystals.

Selected bond lengths (Å) for PbZn(PO$_4$)F (**1**)			
Pb(1)-F(1)#1	2.359(7)	Zn(1)-O(4)#4	1.966(8)
Pb(1)-F(1)	2.504(6)	Zn(1)-F(1)#5	2.097(5)
Pb(1)-O(2)#2	2.469(8)	P(1)-O(1)	1.530(7)
Pb(1)-O(1)#3	2.514(10)	P(1)-O(2)	1.551(8)
Zn(1)-O(1)#3	2.007(6)	P(1)-O(3)	1.515(11)
Zn(1)-O(2)#2	2.023(8)	P(1)-O(4)	1.542(8)
Zn(1)-O(3)	2.005(9)		
Selected bond lengths (Å) for PbSn(PO$_4$)Cl (**2**)			
Pb(1)-Cl(1)	2.830(4)	Sn(1)-O(2)	2.196(9)
Pb(1)-O(1)#1	2.430(8)	Sn(1)-O(3)#3	2.159(8)
Pb(1)-O(1)#2	2.432(8)	P(1)-O(1)	1.530(8)
Pb(1)-O(2)	2.669(8)	P(1)-O(2)	1.538(8)
Pb(1)-O(3)#1	2.707(9)	P(1)-O(3)	1.537(9)
Sn(1)-O(4)#1	2.110(9)	P(1)-O(4)	1.538(9)
Selected bond lengths (Å) for PbSn(PO$_4$)Br (**3**)			
Pb(1)-Br(1)	2.9770(15)	Sn(1)-O(3)#3	2.153(8)
Pb(1)-O(1)#1	2.426(9)	Sn(1)-O(4)#2	2.134(9)
Pb(1)-O(1)#2	2.453(9)	P(1)-O(1)	1.534(10)
Pb(1)-O(2)	2.635(9)	P(1)-O(2)	1.531(9)
Pb(1)-O(3)#2	2.734(8)	P(1)-O(3)	1.550(9)
Sn(1)-O(2)	2.232(9)	P(1)-O(4)	1.525(10)
Selected bond lengths (Å) for PbSn(PO$_4$)I (**4**)			
Pb(1)-I(1)	3.135(2)	Sn(1)-O(3)	2.104(19)
Pb(1)-O(1)	2.700(19)	Sn(1)-O(4)#3	2.15(2)
Pb(1)-O(2)#1	2.44(2)	P(1)-O(1)	1.540(19)
Pb(1)-O(2)#2	2.450(19)	P(1)-O(2)	1.536(19)
Pb(1)-O(4)#2	2.74(2)	P(1)-O(3)#4	1.54(2)
Sn(1)-O(1)	2.210(19)	P(1)-O(4)	1.56(2)

Symmetry transformations used to generate equivalent atoms:

For PbZn(PO$_4$)F (**1**): #1 -x, -y+1, z+1/2 #2 -x+1/2, y-1/2, z+1/2 #3 -x, -y+2, z+1/2 #4 x, y, z+1 #5 -x+1/2, y+1/2, z+1/2.

For PbSn(PO$_4$)Cl (**2**): #1 x, y-1, z #2 -x+2, -y+1, -z+1 #3 -x+1, -y+1, -z+1.

For PbSn(PO$_4$)Br (**3**): #1 -x+2, -y+1, -z+1 #2 x, y-1, z #3 -x+1, -y+1, -z+1.

For PbSn(PO$_4$)I (**4**): #1 -x+1, -y, -z+2 #2 x-1, y, z #3 -x+1, -y, -z+1 #4 x+1, y, z.

Computational method.

The method of plane-wave pseudo-potential (PWPP) of density functional theory (DFT) was used to calculate the electronic structure and optical properties of compounds by running the CASTEP program in the Material Studio software package.[1, 2] By employing the generalized gradient approximation (GGA), the Perdew-Burke-Ernzerhof (PBE) general functional was used to calculate the exchange-correlation potential.[3, 4] The ion nucleus-electron interactions were described by the Norm conserving pseudopotentials (NCP). The valence electrons of the four compounds were set as follows: $Pb-5d^{10}6s^26p^2$, $Sn-5s^25p^2$, $Zn-3d^{10}4s^2$, $P-3s^23p^3$, $O-2s^22p^4$, $F-2s^22p^5$, $Cl-3s^23p^5$, $Br-4s^24p^5$, $I-5s^25p^5$. The cut-off energies of the four compounds (850 eV, 820 eV, 820 eV and 820 eV) under the NCP determined the number of plane waves contained in the basis sets. The four compounds were numerically integrated over the Brillouin zone using Monkhorst-Pack k-point sampling of 3×3×5, 3×5×2, 3×5×2 and 5×3×3.

Table S3. The state energies (eV) of the lowest conduction band (L-CB) and the highest valence band (H-VB) for the four crystals.

Compound	k-point	L-CB (eV)	H-VB (eV)
PbZn(PO$_4$)F	G (0.000 0.000 0.000)	4.478332	-0.01249
	Z (0.000 0.000 0.500)	4.696504	-0.05564
	T (-0.500 0.000 0.500)	4.874404	-0.09792
	Y (-0.500 0.000 0.000)	4.44296	-0.12904
	S (-0.500 0.500 0.000)	4.61555	-0.09943
	X (0.000 0.500 0.000)	4.68196	-0.13624
	U (0.000 0.500 0.500)	4.55085	-0.0038
	R (-0.500 0.500 0.500)	4.865496	-0.05896
PbSn(PO$_4$)Cl	Z (0.000 0.000 0.500)	3.010691	-0.20792
	G (0.000 0.000 0.000)	2.71979	0
	Y (0.000 0.500 0.000)	3.346421	-0.53265
	A (-0.500 0.500 0.000)	3.169945	-0.63279
	B (-0.500 0.000 0.000)	2.728321	-0.29083
	D (-0.500 0.000 0.500)	2.569063	-0.26133
	E (-0.500 0.500 0.500)	2.912721	-0.62013
	C (0.000 0.500 0.500)	3.361783	-0.54616
PbSn(PO$_4$)Br	Z (0.000 0.000 0.500)	3.183517	-0.20721
	G (0.000 0.000 0.000)	2.920716	0
	Y (0.000 0.500 0.000)	3.346633	-0.3243
	A (-0.500 0.500 0.000)	3.190713	-0.47053
	B (-0.500 0.000 0.000)	2.89355	-0.27724
	D (-0.500 0.000 0.500)	2.777096	-0.25666
	E (-0.500 0.500 0.500)	2.926075	-0.4655
	C (0.000 0.500 0.500)	3.394165	-0.32947
PbSn(PO$_4$)I	G (0.000 0.000 0.000)	2.758476	-0.20444
	F (0.000 0.500 0.000)	2.897856	-0.60437
	Q (0.000 0.000 0.500)	2.581096	0
	Z (0.500 0.000 0.000)	2.63994	-0.23483
	G (0.000 0.500 0.500)	2.758476	-0.20444

Table S4. The birefringence of some typical phosphates.

Phosphates' types	Compounds	Space group	Birefringence
Orthophosphates	BPO_4[5]	*I-4*	0.0001@1064nm
	KH_2PO_4[6]	*Im2d*	0.035@1064nm
	$LiCs_2PO_4$[7]	*Cmc2$_1$*	0.01@1064nm
	$KMg(H_2O)PO_4$[8]	*Pmn2$_1$*	0.017@1064nm
	$RbMgPO_4·6H_2O$[9]	*Pmn2$_1$*	0.005@1064nm
	$CsMgPO_4·6H_2O$[9]	*P6$_3$mc*	0.006@1064nm
	$LiPbPO_4$[10]	*Pna2$_1$*	0.021@1064nm
Polyphosphates	$Rb_3BaBi(P_2O_7)_2$[11]	*P2$_1$*	0.025@1064nm
	$Cs_3BaBi(P_2O_7)_2$[11]	*P2$_1$2$_1$2$_1$*	0.025@1064nm
	$K_2PbP_2O_7$[12]	*C2/$_C$*	0.019@1064nm
	$Rb_2PbP_2O_7$[12]	*C2/$_C$*	0.028@1064nm
	$K_4Mg_4(P_2O_7)_3$[13]	*Pc*	0.0108@1064nm
	$KLa(PO_3)_4$[14]	*P2$_1$*	0.008@1064nm
	$CsLa(PO_3)_4$[15]	*P2$_1$*	0.006@1064nm
	$BaPO_3Cl$[16]	*P2$_1$/c*	0.021@1064nm
	$K_2SrP_4O_{12}$[17]	*I-4*	0.016@1064nm
Fluorophosphates	$Cd_{2.5}(NH_4)_2(PO_3F)_3Cl·2H_2O$[18]	*P2$_1$/c*	0.035@546nm
	$Na_{1.5}Rb_{0.5}PO_3F·H_2O$[19]	*Pmn2$_1$*	0.034@546 nm
	$(NH_4)_2Ba(PO_2F_2)_4$[20]	*P2/n*	0.022@1064nm
	$Ba(PO_2F_2)_2$[20]	*I-42d*	0.011@1064nm

Figure S1. Simulated and measured XRD powder patterns of PbZn(PO$_4$)F (a), PbSn(PO$_4$)Br (b) and PbSn(PO$_4$)I (c).
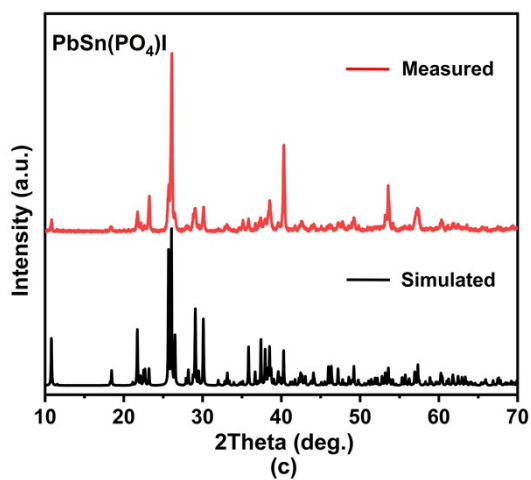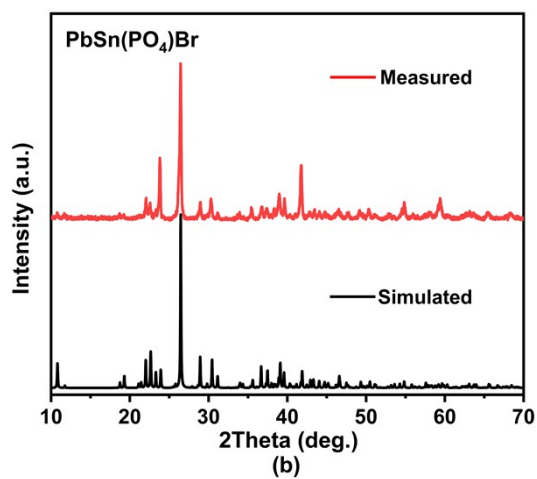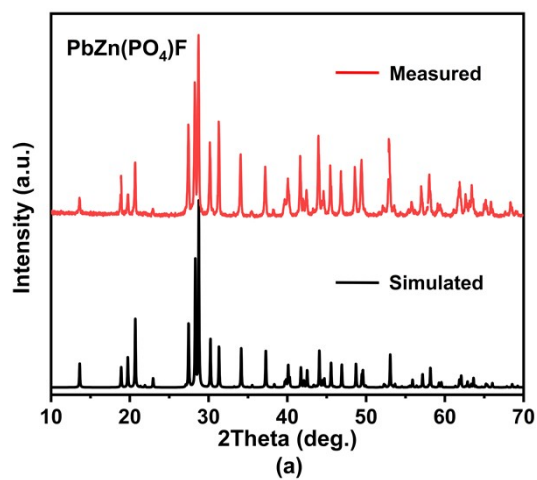
Figure S2. The connection modes of PbO_2F_2 in $PbZn(PO_4)F$.
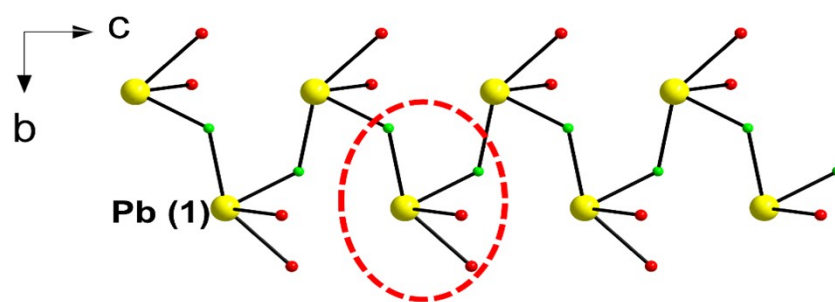
Figure S3. IR spectra of PbZn(PO$_4$)F (a), PbSn(PO$_4$)Br (b) and PbSn(PO$_4$)I (c).
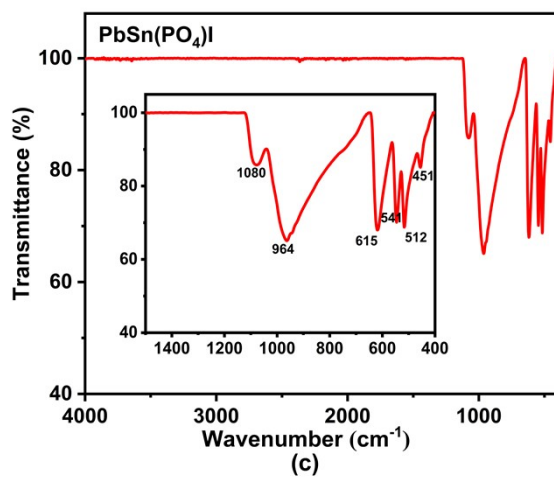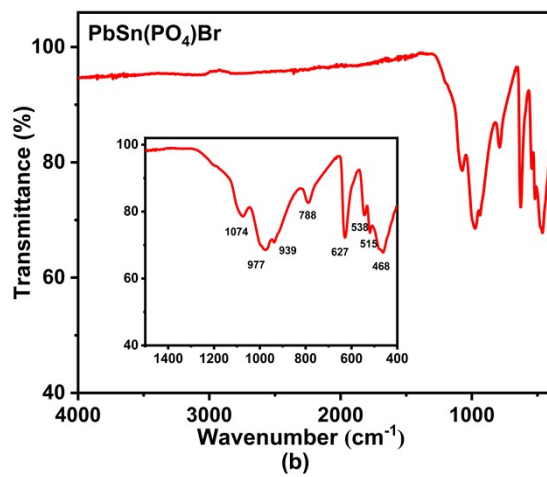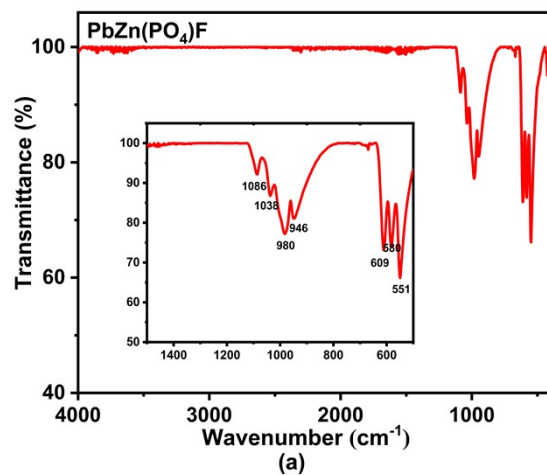
Figure S4. UV−vis−NIR diffuse reflectance spectra of PbZn(PO$_4$)F (a), PbSn(PO$_4$)Br (b) and PbSn(PO$_4$)I (c).
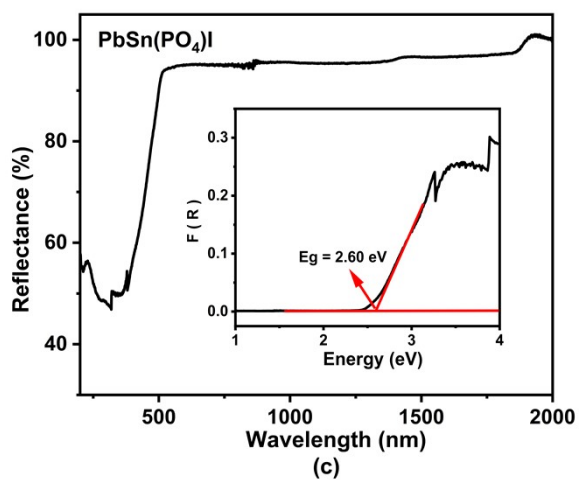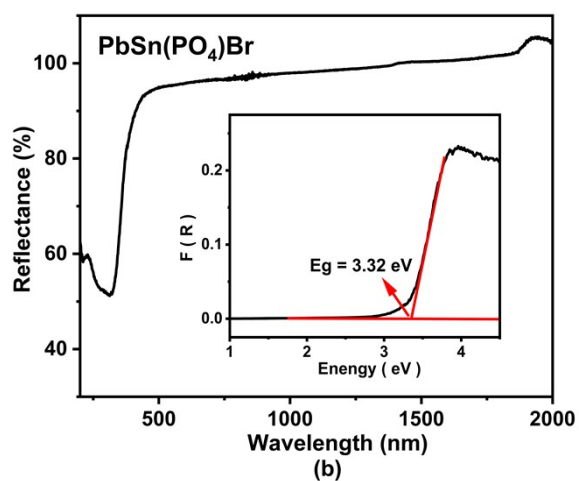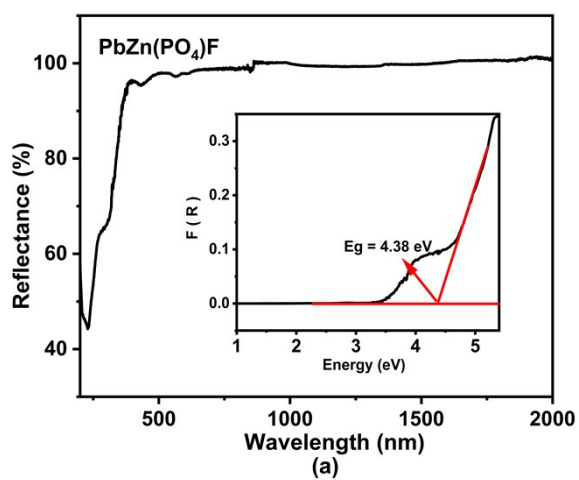
Figure S5. The thermal analysis curves of PbZn(PO$_4$)F, PbSn(PO$_4$)Br and PbSn(PO$_4$)I.
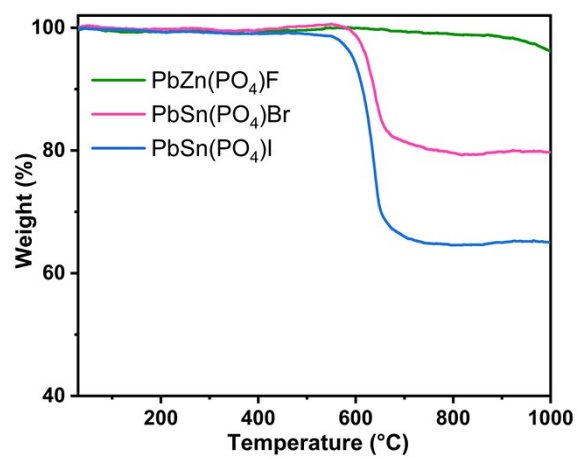
Figure S6. SHG density map of d_{33} in the valence band (left) and the conduction band (right) of $PbZn(PO_4)F$.
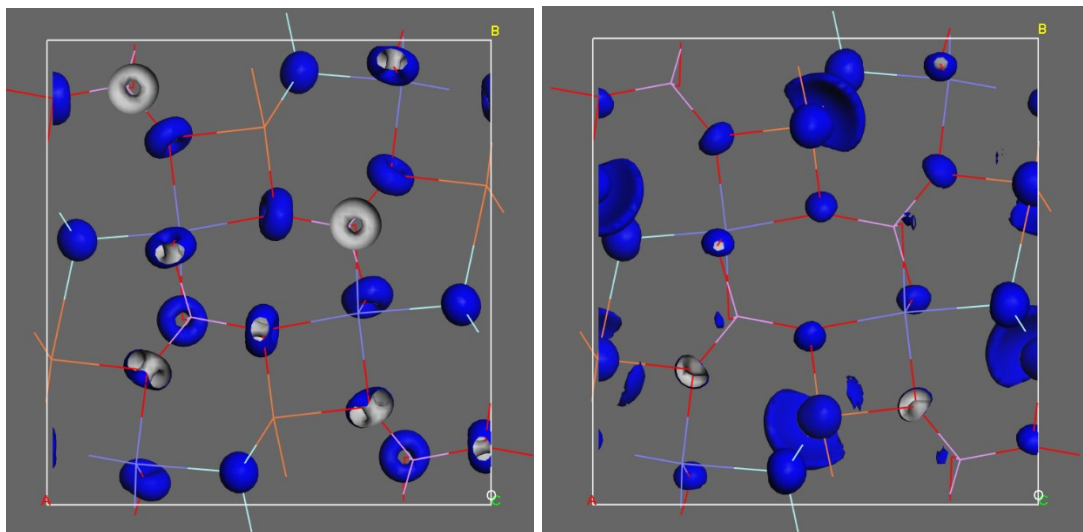
**Figure S7.** The band structures of PbZn(PO$_4$)F (a), PbSn(PO$_4$)Cl (b), PbSn(PO$_4$)Br (c) and PbSn(PO$_4$)I (d).

(a)

(b)

(c)

(d)
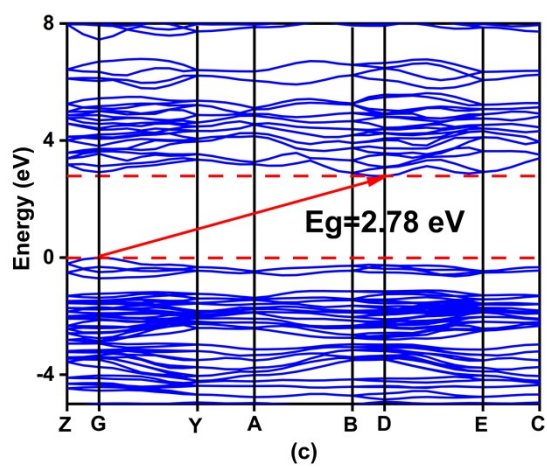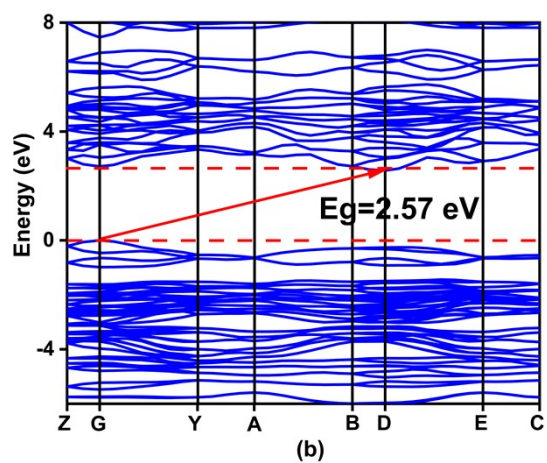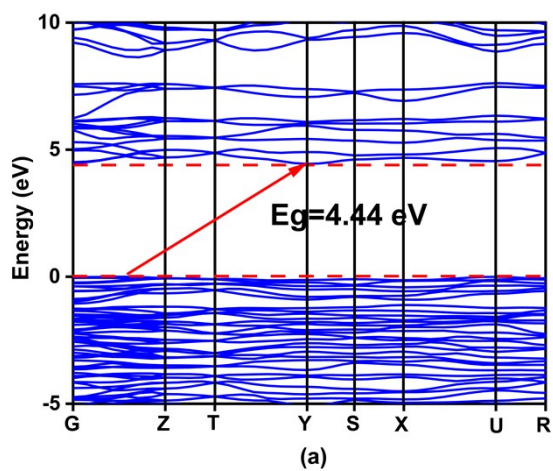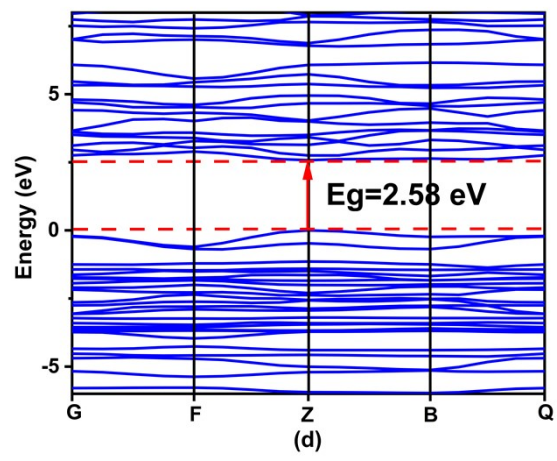
References

1. J. G. S. C. Fonseca Guerra, G. te Velde, E.J. Baerends, Towards an order-N DFT method, *Theor Chem Acc*, 1998, **99**, 391-403.

2. M. D. S. Stewart J. Clark, Chris J. Pickard, Phil J. Hasnip, Matt I. J. Probert, Keith Refson and Mike C. Payne, First principles methods using CASTEP, *Z Kristallogr Cryst Mater*, 2005, **220**, 567-570.

3. J. S. Lin, A. Qteish, M. C. Payne and V. V. Heine, Optimized and transferable nonlocal separable ab initio pseudopotentials, *Phys. Rev., B Condens Matter*, 1993, **47**, 4174-4180.

4. K. B. John P. Perdew, Matthias Ernzerhof, Generalized Gradient Approximation Made Simple., *Phys. Rev. Lett.*, 1996, **77**, 3865-3868.

5. Z. L. Zhihua Li, Yicheng Wu, Peizhen Fu, Zhizhong Wang, and Chuangtian Chen, Crystal Growth, Optical Properties Measurement, and Theoretical Calculation of BPO_4, *Chem. Mater.*, 2004, **16**, 2906-2908.

6. J. Kobayashi, T. Takahashi, T. Hosokawa and Y. Uesu, A new method for measuring the optical activity of crystals and the optical activity of KH_2PO_4, *J. Appl. Phys.*, 1978, **49**, 809-815.

7. L. Li, Y. Wang, B. H. Lei, S. Han, Z. Yang, K. R. Poeppelmeier and S. Pan, A New Deep-Ultraviolet Transparent Orthophosphate $LiCs_2PO_4$ with Large Second Harmonic Generation Response, *J. Am. Chem. Soc.*, 2016, **138**, 9101-9104.

8. Z. Bai, C.-L. Hu, L. Liu, L. Zhang, Y. Huang, F. Yuan and Z. Lin, $KMg(H_2O)PO_4$: A Deep-Ultraviolet Transparent Nonlinear Optical Material Derived from $KTiOPO_4$, *Chem. Mater.*, 2019, **31**, 9540-9545.

9. Y. Zhou, L. Cao, C. Lin, M. Luo, T. Yan, N. Ye and W. Cheng, $AMgPO_4 \cdot 6H_2O$ (A = Rb, Cs): strong SHG responses originated from orderly PO_4 groups, *J. Mater. Chem. C*, 2016, **4**, 9219-9226.

10. G. Han, Q. Liu, Y. Wang, X. Su, Z. Yang and S. Pan, Experimental and theoretical studies on the linear and nonlinear optical properties of lead phosphate crystals $LiPbPO_4$, *Phys. Chem. Chem. Phys.*, 2016, **18**, 19123-19129.

11. L. Qi, Z. Chen, X. Shi, X. Zhang, Q. Jing, N. Li, Z. Jiang, B. Zhang and M.-H. Lee, $A_3BBi(P_2O_7)_2$ (A = Rb, Cs; B = Pb, Ba): Isovalent Cation Substitution to Sustain Large Second-Harmonic Generation Responses, *Chem. Mater.*, 2020, **32**, 8713-8723.

12. M. Wen, H. Wu and X. Wu, Influence of Cation on the Anion Frameworks and Properties of Four Lead Phosphates, $A_2PbBi_2(PO_4)_2(P_2O_7)$ (A = Rb, Cs) and $A_2PbP_2O_7$ (A = K, Rb), *Inorg. Chem.*, 2020, **59**, 2945-2951.

13. H. Yu, J. Young, H. Wu, W. Zhang, J. M. Rondinelli and P. S. Halasyamani, $M_4Mg_4(P_2O_7)_3$ (M = K, Rb): Structural Engineering of Pyrophosphates for Nonlinear Optical Applications, *Chem.. Mater.*, 2017, **29**, 1845-1855.

14. P. Shan, T. Sun, H. Chen, H. Liu, S. Chen, X. Liu, Y. Kong and J. Xu, Crystal growth and optical characteristics of beryllium-free polyphosphate, $KLa(PO_3)_4$, a possible deep-ultraviolet nonlinear optical crystal, *Sci. Rep.*, 2016, **6**, 25201.

15. T. Sun, P. Shan, H. Chen, X. Liu, H. Liu, S. Chen, Y. a. Cao, Y. Kong and J. Xu, Growth and properties of a noncentrosymmetric polyphosphate $CsLa(PO_3)_4$ crystal with deep-ultraviolet transparency, *CrystEngComm*, 2014, **16**, 10497-10504.

16. J. Feng, C. L. Hu, Y. Lin and J. G. Mao, $BaPO_3Cl$: a Metal Phosphate Chloride with Infinite $[PO_3]_\infty$ Chains, *Inorg. Chem.*, 2019, **58**, 73-76.

17. Z. Bai, L. Liu, L. Zhang, Y. Huang, F. Yuan and Z. Lin, $K_2SrP_4O_{12}$: a deep-UV transparent cyclophosphate as a nonlinear optical crystal, *Chem. Commun. (Camb.)*, 2019, **55**, 8454-8457.

18. X. R. Yang, X. Liu, L. Chen and L. M. Wu, A deep ultraviolet transparent birefringent monofluorophosphate: $Cd_{2.5}(NH_4)_2(PO_3F)_3Cl \cdot 2H_2O$, *Z Anorg Allg Chem*, 2022, **648**.

19. X.-R. Yang, X. Liu, Z. Wang, X.-B. Deng, H.-J. Lu, Y.-J. Li, X. Long, L. Chen and L.-M. Wu, $Na_{1.5}Rb_{0.5}PO_3F \cdot H_2O$: synthesis, properties, and stepwise reconstruction of the hydrogen bond network, *Inorg. Chem. Front.*, 2021, **8**, 4544-4552.

20. W. Zhang, W. Jin, M. Cheng, R. Zhang, Z. Yang and S. Pan, From centrosymmetric to noncentrosymmetric: effect of the cation on the crystal structures and birefringence values of $(NH_4)_{n-2}AE(PO_2F_2)_n$ (AE = Mg, Sr and Ba; n = 2, 3 and 4), *Dalton Trans.*, 2021, **50**, 10206-10213.